DOI: https://doi.org/10.37434/tpwj2024.12.07

STUDIES OF EDDY CURRENT PROBES FOR INSPECTION OF ALUMINIUM ALLOY STRUCTURE WELDS USING SMARTPHONE-BASED FLAW DETECTOR

G. Mook[1], **V. Uchanin**[2], **Ju. Lysenko**[2]

[1]Otto-von-Guericke-Universität Magdeburg, Universitätsplatz 2, 39106 Magdeburg, Germany
[2]G.V. Karpenko Physico-Mechanical Institute of the NASU
5 Naukova Str., 79060, Lviv, Ukraine
[3]National Technical University of Ukraine "Igor Sikorsky Kyiv Polytechnic Institute"
37 Prosp. Beresteiskyi, 03056, Kyiv, Ukraine

ABSTRACT

Features of the design and capabilities of the smartphone-based eddy current flaw detector with the EddySmart software application are presented, which in the future can provide a remote inspection with the wireless transmission of inspection results via mobile communication channels for the further analysis and storage. The perspectives of application of eddy current probes (ECP) of double differential type for inspection of structure welds made of aluminium alloys are considered. The characteristics and results of studies of low-frequency double differential MDF 0801 and MDF 1001M type eddy current probes with operational diameters of 8 and 10 mm, respectively, designed for detection of defects in aluminium alloy welds are presented. It is shown that to detect extended and local defects in aluminium alloy structure welds at a greater depth, the preference should be given to the improved eddy current probe of MDF 1001M type with an operational diameter of 10 mm, which provides a higher level of signals and better noise resistance.

KEYWORDS: non-destructive inspection, eddy current probe, smartphone-based flaw detector, weld, aluminium alloy

INTRODUCTION

Today, pocket smartphones have become an integral part of our live. Smartphones differ from conventional mobile phones in that they have a full-fledged operating system open to software development, unlike mobile phones that have a closed operating system. In addition, smartphones have the features of a personal computer with permanent data storage, random-access memory and relatively powerful central and graphics processors. A modern smartphone can have a variety of sensors (including accelerometer, gyroscope, magnetometer, light sensor, barometer, thermometer, Hall sensor and fingerprint scanner), which improves its functional versatility and the ability of using it not only for communication or entertainment. The use of a smartphone as a measuring device is somewhat unconventional. There are examples of creating a fully functioning microscope based on a smartphone using a rubber attachment for a camera with a 1 mm diameter lens. The resolution of such a microscope was about 1.5 μm. Another interesting example is the implementation of a smartphone-based spectrometer for analysing light waves.

There are also examples of the implementation of smartphone-based full-fledged systems of non-destructive inspection (NDI), technical diagnostics and monitoring [1–9]. In [1–3] an ultrasonic flaw detector, created at the Igor Sikorsky Kyiv Polytechnic Institute is described, which consists of an electronic unit with an ultrasonic sensor and a smartphone. The exchange of information between the sensor unit and the smartphone is performed via wireless networks using Bluetooth technology. The flaw detector operation algorithm is implemented using special software that runs on the Android operating system. A similar approach is implemented in the development of the French Company LECOEUR ELECTRONIQUE [4]. Another example concerns a system for vibration monitoring of the technical condition of structures [5]. The authors have developed a system application for Android that can easily turn several smartphones into a wireless vibration monitoring system for structures. A server-client architecture was used, where one smartphone is designated as a remote control system for all other smartphones, allowing the server smartphone to quickly and easily connect multiple smartphones with sensors to create a wireless network. A method for synchronising different smartphones to simultaneously measure the vibration of structures was also proposed.

A successful implementation of a smartphone-based NDI device is an eddy current flaw detector (ECFD) with the EddySmart application, which has been successfully used primarily for student education [10, 11]. But already today, the ambitions of this development go beyond the tasks defined at the initial stage of its creation. In [12], it is considered

as a sprout for the creation of promising technologies within the framework of the NDI 4.0 concept. The authors, in particular, draw attention to the possibility of wireless transmission of inspection results via mobile communication channels for the further analysis and storage. The smartphone-based ECFD with the EddySmart application was effectively used to demonstrate the capabilities of new eddy current technologies for detection of inner defects in aircraft and space structures, which eliminated the need in using bulky traditional ECFDs.

Low-frequency double differential eddy current probes (ECPs) have been widely used to detect surface and inner defects in structures made of nonmagnetic materials [13]. Their peculiarity is high sensitivity to local defects compared to traditional ECPs. Therefore, double differential ECPs are promising for creating technologies for detecting weld defects, especially when inspection becomes more complicated due to noise signals created by the inhomogeneity of the specific electrical conductivity and changes in geometry (reinforcement bead, edge warping, etc.) in the weld zone. Here, it is necessary to use signal interpretation methods applying the ECFD's integrated display plane [14]. Double differential ECPs have already found their use, including for the detection of lacks of fusion and pores in welds [15, 16]. In the extended welds of the shells in space structures of aluminium 1201 alloy made by electron beam welding, surface defects of lack of fusion (adhesion) type were successfully detected. Defects of this type can be formed when the electron beam deviates from the butt of parts to be welded. Due to the partial diffusion bonding (adhesion) of welded edges, this type of defect is extremely difficult to detect using conventional NDI methods. Another example concerns the problem of detecting welded surface and inner defects of various types in the welds of space structures made of AMg-5 and AMg-6 type alloys, produced by arc welding. Inspection technologies based on the use of low-frequency ECPs ensured the detection of not only surface defects, but also subsurface defects such as pores, lacks of fusion, inclusions and oxide films, despite the lift-off created by the inhomogeneity of the weld geometry. The results of the further studies have shown the possibility of improving and optimizing the ECP for welds inspection in order to reduce the sizes of the ECP with a corresponding improvement in the resolution, at the same time increasing the depth of inspection, which will allow detecting extended and local defects at a greater depth.

This work presents the features of the design and capabilities of a smartphone-based ECFD and studies carried out by improved low-frequency double-differentiation ECPs for detecting inner defects in welds of aluminium alloy.

1. DESIGN, MAIN FUNCTIONS AND CAPABILITIES OF A SMARTPHONE-BASED EDDY CURRENT FLAW DETECTOR

Let us consider the main functions that need to be implemented to create a smartphone-based ECFD using a generalized block diagram of a typical ECFD (Figure 1). The creation of a primary sinusoidal electromagnetic field of the required operating frequency is performed by a controlled generator *1* and a power amplifier *2*, which provide the required current level in the ECP generator winding *3*, which interacts with the test object (TO) *4*, inducing eddy currents in it. The resulting electromagnetic field of the TO *4* generates a signal in the measuring ECP winding *3*, which carries components caused by the unbalance of the ECP (signal of the measuring winding during its placing on a defect-free part of the TO) and the influence of a defect in the TO during scanning of its surface. The appearance of a defect during scanning changes the distribution of eddy currents, which affects the ECP input signal, performing modulation of the output ECP signal at the operating frequency. The ECP output signal is fed to the input cascade *5*, which provides its improvement by amplification to the required level and HF-filtering. Then the signal is fed to phase-sensitive detectors *6* and *7*, which perform the

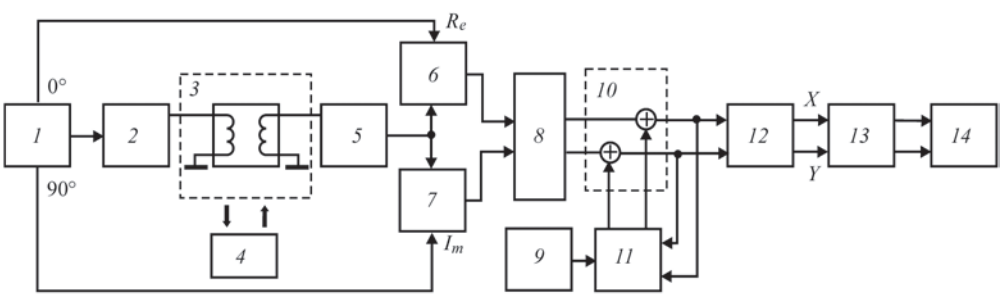

Figure 1. Block diagram of a typical ECFD composition: *1* — generator; *2* — power amplifier; *3* — ECP; *4* — TO; *5* — input cascade; *6* and *7* — phase-sensitive rectifiers; *8* — filters; *9* — adder; *10* — circuit for unbalance compensation signal formation with a start button *11*; *12* — phase shifter; *13* — amplifier of *X* and *Y* components; *14* — display

ECP signal demodulation operation, generating DC signals at the output corresponding to real and imaginary components of the ECP output signal. Further, the output signals of phase-sensitive detectors *6* and *7* through filters *8* are fed to adders *9* for compensation of the ECP unbalance, the other input of which receives the signals necessary for compensation of unbalance from the unbalance compensation signal generation circuit *10* with a start button *11*. To reduce the noise influence, low-pass (LP) or high-pass (HP) filters with adjustable cutoff frequencies are used. When both filters are used simultaneously, a band-pass filter mode is provided. To compensate for the ECP unbalance signal, the ECP is placed on a defect-free part of the sample, and then the operator starts the balancing process by pressing the button *11*. Thus, real and imaginary components of the signal eliminate the components, corresponding to the ECP position on a defect-free part of the sample (TO). This operation allows selecting components that correspond only to the defect influence. Then, the obtained components are fed to the phase shifter *12*, which rotates the complex plane of the ECFD by an angle of 0–360°, which allows manipulating the signal hodographs in the complex plane of the ECFD during scanning of the TO surface, directing the useful signal, for example, in the vertical direction of the display. From the output of the phase shifter *12* through the amplifier *13*, the horizontal *X* and vertical *Y* components are fed to the ECFD display, which displays changes in the ECP signal in the complex plane (*Y/X* mode) or changes in real or imaginary components of the ECP signal in the time scan mode (*Y/t* or *X/t* mode).

A modern smartphone contains all the components required for building an eddy current device with the above functions (Figure 1). Its audio interface allows simultaneous transmission and reception of signals with a frequency of up to 20 kHz, which is sufficient for operation in the low-frequency range of eddy current inspection. Thus, the main idea of the development is to use the audio system of a smartphone to build an eddy current device, unlike ultrasonic smartphone-based systems, when the units necessary for creating a flaw detector (in particular, generators and signal processing circuit elements) are made in a separate unit [10, 11]. In this case, ECPs are connected directly to the smartphone's audio jack, which provides a signal strong enough for its operation, where additional power amplifier is not required. The quality of the 4-pin audio jack plays an important role, so it is necessary to choose a version with gold-plated contacts. For such a connection, the ECP cable is equipped with an electronic circuit that simulates a headset. The flaw detector designed by the Otto von Guericke University Magdeburg requires the use of an Android OS smartphone, in particular, of the Samsung Galaxy series.

The generalized structure of the EddySmart software application is shown in Figure 2, which also shows the correspondence of the displayed control results and adjustment operations to different areas of the smartphone touch screen. Hence, it is seen, that most of the functions of the ECFDs shown in Figure 1, are implemented by the software.

The background process simultaneously processes the ECP signal buffers (output excitation and input measurement). It fills the two-channel buffer with a sinusoidal excitation signal and empties the single-channel input signal buffer, which contains a mixture of excitation and measurement signals. The measurement signal is separated in the received signal and demodulated with respect to the ECP excitation signal. This process is implemented without participation of the user (flaw detector operator).

The user interface provides indication of inspection results, amplification to intensify the obtained

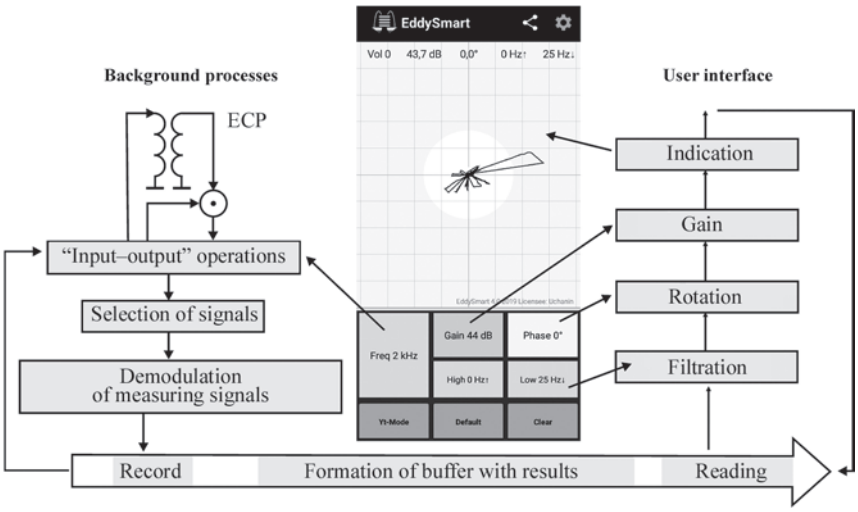

Figure 2. Generalized structure and appearance of the EddySmart software application display

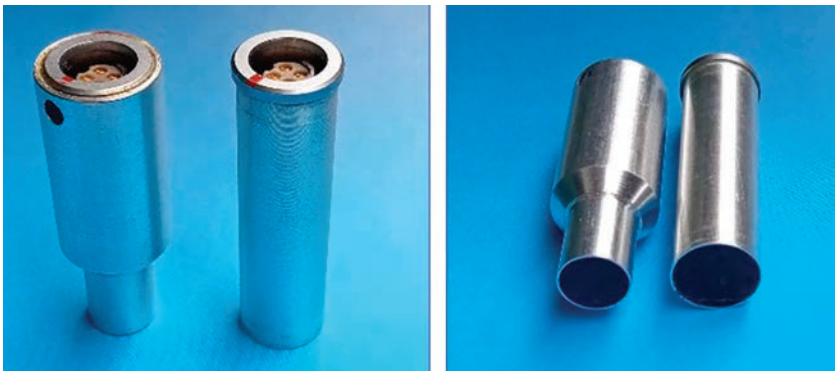

Figure 3. Studied double differential MDF 0801 and MDF 1001M type ECPs

hodographs and their rotation in the complex plane, as well as filtering. The selection of these parameters is controlled by the flaw detector operator using the touch screen of a smartphone.

The upper line of the smartphone display shows the audio signal level, which is adjusted by the corresponding smartphone button, as well as the gain level, complex frequency rotation angle and cutoff frequencies of the LP- and HP-filters. Most of the smartphone display is used to indicate the inspection results, which can reflect hodorgaphs of the signals from defects in the complex plane or changes in the signal from a defect in the time scan mode. This part of the display is also used to adjust the gain and rotation of the complex plane by means of manipulations easy to understand for the operator [10, 11]. The lower third of the touch screen display is used to select modes and inspection parameters using the corresponding buttons, including selection of the operating frequency (Freq — upper left), switching to the time scan mode (Yt-mode — lower left), switching on the gain (Gain dB — upper in the middle line), selection of the high-pass filter cut-off frequency (High Hz — middle), default operation (Default — lower in the middle line), phase selection (Phase — upper in the right line), selection of low-pass filter cut-off low frequency (Low Hz — middle in the right line) and selection of screen record or clear mode (Record or Clear — lower in the right line).

The presented capabilities of a smartphone-based ECFD allow it to be used to select the optimal operating frequency and study the sensitivity of ECP to various types of subsurface defects.

2. STUDY OF LOW-FREQUENCY DOUBLE DIFFERENTIAL ECPS FOR DETECTION OF WELD DEFECTS IN ALUMINIUM ALLOY STRUCTURES

2.1. STUDIED ECPs, SAMPLES AND RESEARCH TECHNIQUES

Experimental prototypes of two low-frequency double differential MDF 0801 and MDF 1001M type ECPs with the working surface diameters of 8 and 10 mm, respectively (Figure 3), designed to detect defects in welds of aluminium alloys were studied. The peculiarity of the MDF 0801 type ECP is the higher resolution required to detect not only extended defects such as cracks, but also local defects of a sufficiently small diameter such as pores or inclusions. The advantage of the MDF 1001M type ECP is an increased depth of inspection due to an increased winding diameter. The parameters of the experimental ECPs are given in Table 1, where: D_{ECP} is the ECP diameter; D_f is the ferrite core diameter; w_{ew} and w_{mw} are the quantity of turns of excitation and measuring windings, respectively; L_{ew} and L_{mw} are the inductances of excitation and measuring windings, respectively.

To study the influence of the flaw depth, regardless of its size, assembled standard specimens (SS) were used, each of which allows simulating a defect of the same depth for two discrete values of the flaw depth (Figure 4). Two SS parts are assembled in such a way that after their combination, a rectangular plate of a thickness T is formed with the buttt of the two parts perpendicular to the SS surface, which reproduces a subsurface defect of a depth a. From the different SS surface, the flaw depths of a defect h_{f1} and h_{f2} are different according to the ratio $h_{f1} + h_{f2} + a = T$. Two SSs made of aluminium D16 T alloy were used for

Table 1. Parameters of studied ECPs

ECP type	D_{ECP}, mm	D_f, mm	w_{ew}	w_{mw}	L_{ew}, μH	L_{mw}, μH
MDF 0801	8.0	1.85	215	416	940	3.7
MDF 1001M	10.0	2.9	125	420	310	1.4

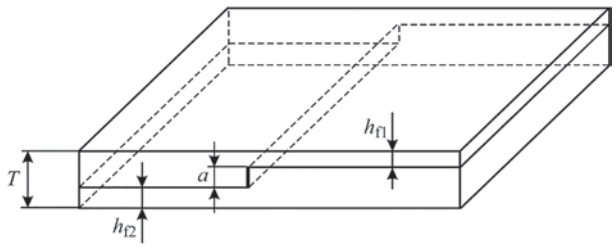

Figure 4. Assembled SS for reproduction of two discrete values of defect flaw depth

the studies, the parameters of which are presented in Table 2.

Thus, the presented SSs allow obtaining four discrete values (1.0, 2.0, 3.0 and 4.0 mm) of the flaw depth of location for a subsurface crack-type defect of the same size and studying the influence of the flaw depth of location on the ECP signal regardless of defect sizes.

2.2. COMPARATIVE ANALYSIS OF ECP SIGNALS FROM SUBSURFACE DEFECTS

Figure 5 shows the MDF 0801 type ECP signals from SS defects with different flaw depths in the complex plane at an operating frequency of 2 kHz, which turned out to be optimal for these defects.

Figure 6 shows the MDF 1001M type ECP signals from SS defects with different flaw depths in the complex plane at an operating frequency of 2 kHz.

The analysis of the ECP signals in Figures 5 and 6 shows that the MDF 0801 and MDF 1001M type ECPs allow detecting all SS defects with a flaw depth of up to 4 mm, although for both ECPs the amplitude of the signals from defects significantly decreases with an increase in their flaw depth. Simultaneously with an increase in the flaw depth, the direction of the hodograph from a defect (signal phase) in the complex plane expands clockwise, which can be used to determine the flaw depth in the future. At the same time, the MDF 0801 type ECP requires more signal amplification. In particular, to detect a defect with a depth of 4 mm by the MDF 0801 type ECP, 70 dB amplification is required, and only 56 dB is required when using the MDF 1001M type ECP. This indicates that the MDF 1001M type ECP has greater capabilities when it is required to detect subsurface defects, since the level of noise grows with an increase in amplification, as is seen from the comparison of signals in Figures 3 and 4. However, it should be kept in mind that the MDF 0801 type ECP may have a potential advantage in terms of resolution and the ability to detect local defects of smaller size due to the significantly smaller diameter of the used ferrite cores (see Table 1).

Table 2. SS parameters for studying the influence of flaw depth of location

SS type	SS thickness *T*, mm	Flaw depth α, mm	Flaw depth of location, mm	
			h_{f1}	h_{f2}
SOP 7.2.2-3	7.0	2.0	2.0	3.0
SOP 7.2.1-4			1.0	4.0

To study the signals from subsurface local defects, a 6 mm thick plate of D16 T aluminium alloy with two

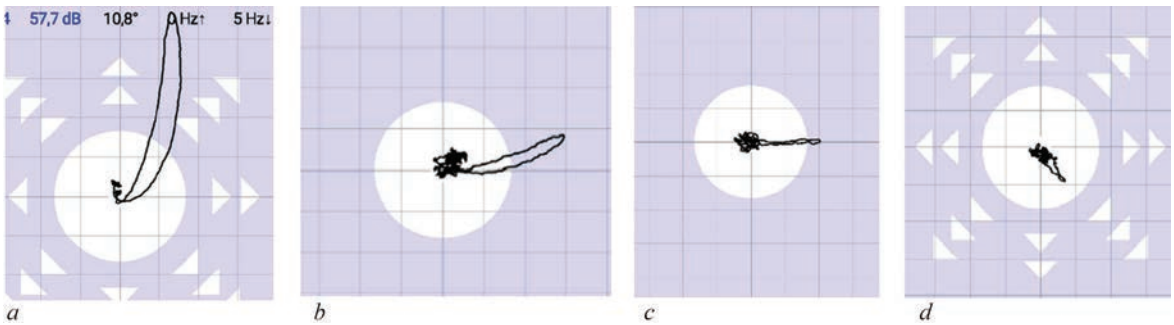

Figure 5. Signals of the MDF 0801 type ECP at an operating frequency of 2 kHz from SS defects (Figure 2) with a flaw depth of location, mm: 1 (*a*); 2 (*b*); 3 (*c*), 4 (*d*); gain ratio for defects with different flaw depths of location, dB: 58 (*a*); 64 (*b*); 70 (*c*, *d*)

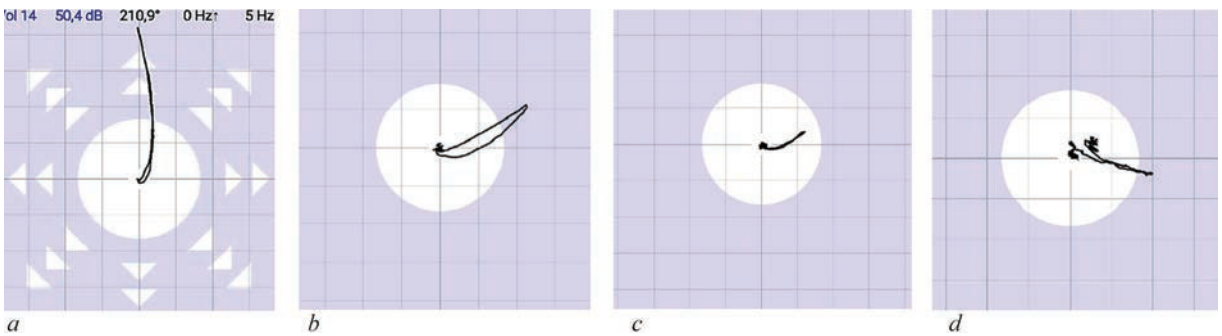

Figure 6. Signals of the MDF 1001M type ECP at an operating frequency of 2 kHz from SS defects (Figure 2) with a flaw depth of location, mm: 1 (*a*); 2 (*b*); 3 (*c*), 4 (*d*); gain ratio for defects with different flaw depth of location, dB: 50 (*a*); 56 (*b*–*d*)

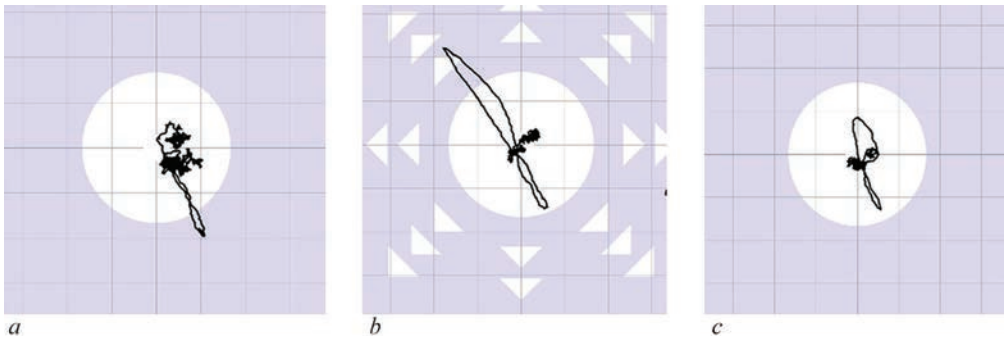

Figure 7. Signals of MDF 0801 (*a*) and MDF 1001M type ECP (*b*, *c*) at an operating frequency of 2 kHz from subsurface local defects of 1.0 mm diameter with a flaw depth of location of 0.6 mm (*a*, *b*) and 1.0 mm (*c*); gain ratio for defects with different flaw depth of location, dB: 66 (*a*); 62 (*b*, *c*)

flat-bottomed holes of 1.0 mm in diameter at different depths was used to simulate subsurface local defects with a flaw depth of location of 0.6 and 1.0 mm. The corresponding signals for the MDF 0801 and MDF 1001M type ECPs at an operating frequency of 2 kHz are shown in Figure 7.

The obtained signals (Figure 7) show that the MDF 0801 and MDF 1001M type ECPs provide detection of a local defect with a diameter of 1 mm. However, the ECP of MDF 0801 type allows identifying only a defect with a flaw depth of location of 0.6 mm (Figure 7, *a*). At the same time, here the signal from a defect is distorted by a high level of noise compared to the signal of the MDF 1001M ECP type from the same defect (Figure 7, *a*).

Summing up the results obtained in Figures 6, 7, it should be noted, that if it is necessary to detect extended and local defects at a greater depth, the preference should be given to the improved MDF 1001M type ECP, which provides a higher level of signals generated by subsurface defects and better noise resistance.

CONCLUSIONS

The features of the design and capabilities of a smartphone-based eddy current flaw detector with the EddySmart application are considered, which in the future can provide remote inspection with wireless transmission of inspection results via mobile communication channels for the further analysis and storage. The prospects for the use of double differential eddy current probes for the inspection of aluminium alloy structure welds were analyzed. The characteristics and results of studies of low-frequency double differential MDF 0801 and MDF 1001M type ECPs with working surface diameters of 8 and 10 mm, respectively, designed to detect defects in welds of aluminium alloys are presented. It is shown that to detect extended and local defects in welds of aluminium alloy structures at a greater depth, the preference should be given to the improved ECP of the MDF 1001M type, which provides a higher signal level and better noise resistance.

REFERENCES

1. Petryk, V., Protasov, A., Galagan, R. et al. (2020) Smartphone-based automated non-destructive testing devices. *Devices and Methods of Measurements,* 11(**4**), 272–278. DOI: https://doi.org/10.21122/2220-9506-2020-11-4-272-278
2. Petryk, V., Protasov, A., Syeryy, K., Povshenko, O. (2019) Use of serial mobile devices in design of portable flaw detectors. *Vcheni Zapysky TNU, Seriya: Tekhnichni Nauki,* 6(**2**), 12–16 [in Ukrainian]. DOI: https://doi.org/10.32838/2663-5941/2019.6-2/03
3. Petryk, V., Protasov, A., Syeryy, K., Ukrainec, S. (2017) Wireless data transmission in ultrasonic nondestructive testing. *Scientific Proc. of STUME, NDT Days 2017*, *Sozopol*, 216(**1**), 121–123.
4. https://www.lecoeur-electronique.net/us-web.html
5. Zhang, D, Tian, J, Li, H. (2020) Design and validation of android smartphone based wireless structural vibration monitoring system. *Sensors*, 20(**17**), 4799. DOI: https://doi.org/10.3390/s20174799
6. Xie, B., Li, J., Zhao, X. (2019) Research on damage detection of a 3D steel frame model using smartphones. *Sensors,* 19(**3**), 745–762. DOI: https://doi.org/10.3390/s19030745
7. Yu, Y., Han, R., Zhao X. et al. (2015) Initial validation of mobile-structural health monitoring method using smartphones. *Inter. J. of Distributed Sensor Networks,* 11(**2**), 1–14. DOI: https://doi.org/10.1155/2015/274391
8. Meiqin, Z., Weiguo, G., Zhenghao, L., Liu-yang, Z. (2007) Design of remote monitoring system for household applicances and home security based on smartphone. *Measurement and Control Technology*, 26(**8**), 72–75.
9. Felice, M., Heng, I., Udell, C., Tsalicoglou, I. (2021) Improving the productivity of ultrasonic inspections with digital and mobile technologies. In: *Proc. of Conf. on NDE 2019*, *Dec 5–7, Bengaluru, India*. https://www.ndt.net/article/nde-india2019/papers/CP227
10. Mook, G., Simonin, Y. (2018) Eddy current notebook and smartphone. In: *Proc. of 14th Inter. Conf. of the Slovenian Society for NDT*, *Sep 4–6, 2017, Bernardin, Slovenia*. https://www.ndt.net/article/ndt-slovenia2017/papers/135.pdf
11. Mook, G., Simonin, Y. (2018) Smartphone turns into eddy current instrument. In: *Proc. of 12th Europ. Conf. on NDT*, *Gothenburg, Sweden, June 11–15*. https://www.ndt.net/article/ecndt2018/papers/ecndt-0079-2018.pdf
12. Udell, C., Maggioni, M., Mook, G., Meyendorf, N. (2022) *Improving NDE 4.0 by networking, advanced sensors, smartphones, and tablets*: Handbook of Nondestructive Evaluation 4.0. Springer, Cham. Eds by N. Meyendorf, N. Ida, R. Singh, J. Vrana. DOI: https://doi.org/10.1007/978-3-030-73206-6_53

13. Uchanin, V. (2023) Surface eddy current probes of double differential type as an effective tool to solve non-destructive inspection problems. *The Paton Welding J.*, **2**, 46–55. DOI: https://doi.org/10.37434/tpwj2023.02.07
14. DSTU ISO 17643:2015: *Non-destructive testing of welds. Eddy current testing of welds by complex-plane analysis*.
15. Uchanin, V. (2008) Eddy current testing of welded joints. *Tekh. Diagnost. i Nerazrush. Kontrol*, **4**, 71–80 [in Russian].
16. Uczanin, W. (2013) Badania nieniszczące złączy spawanych z wykorzystaniem metody prądów wirowych. *Przegląd Spawalnictwa,* 85(**7**), 25–33 [in Polish].

ORCID
V. Uchanin: 0000-0001-9664-2101,
Ju. Lysenko: 0000-0001-9110-6684

CONFLICT OF INTEREST
The Authors declare no conflict of interest

CORRESPONDING AUTHOR
V. Uchanin
G.V. Karpenko Physico-Mechanical Institute of the NASU
5 Naukova Str., 79060, Lviv, Ukraine.
E-mail: vuchanin@gmail.com

SUGGESTED CITATION
G. Mook, V. Uchanin, Ju. Lysenko (2024) Studies of eddy current probes for inspection of aluminium alloy structure welds using smartphone-based flaw detector. *The Paton Welding J*., **12**, 42–48.
DOI: https://doi.org/10.37434/tpwj2024.12.07

JOURNAL HOME PAGE
https://patonpublishinghouse.com/eng/journals/tpwj

Received: 05.07.2024
Received in revised form: 24.09.2024
Accepted: 26.12.2024